Int. J. Heat Mass Transfer. Vol. 28, No. 3, pp. 547–552, 1985
Printed in Great Britain

0017-9310/85 $3.00 + 0.00
Pergamon Press Ltd.

Critical heat flux in saturated forced convective boiling on a heated disk with an impinging jet—CHF in *L*-regime

MASANORI MONDE and YOSHIAKI OKUMA
Department of Mechanical Engineering, Saga University, Japan

(*Received* 29 *February* 1984)

Abstract—An experimental study of critical heat flux (CHF) has been made for a saturated forced convective system at atmospheric pressure: a liquid is supplied through a small round jet of water or R113, setup upwards below a heated disk. The experiments have been carried out for a velocity of $u = 0.33$ to 13.7 m/s and a diameter ratio of $D/d = 9.6$ to 57.1. The CHF, which takes place in the present experimental range, is divided into two different characteristic regimes (*L*- and *V*-regimes) depending on the jet velocity, the diameter ratio and the jet diameter. The CHF in the *L*-regime, namely at the rather small velocity and the large diameter ratio, which was guessed to appear but was not proved experimentally, is not only obtained in the present experiment, but also predicted by a generalized correlation with a good accuracy.

1. INTRODUCTION

MANY STUDIES of critical heat flux (CHF) have been made for a saturated forced convection boiling on an open heated disk being fed with a liquid by means of a small round jet [1–9].

Monde [10] recently proposes a successful correlation (1) of CHF data in the *V*-regime for saturated liquid jet impinging on the heated disks.

$$\frac{q_{co}}{\rho_v H_{fg} u} = 0.221\left(\frac{\rho_l}{\rho_v}\right)^{0.645} \times \left(\frac{2\sigma}{\rho_l u^2 (D-d)}\right)^{0.343} (1+D/d)^{-0.364}. \quad (1)$$

However, in the special case that the diameter ratio of the heated disk to the jet diameter, D/d, becomes very large and in addition the jet velocity becomes very small, another type of the CHF seems to take place [3, 4, 7]. As the result, equation (1) would not predict the CHF data for such a situation, although few CHF data in the *L*-regime have been measured until now.

The present study, therefore, involves an experiment employing water and R113 at atmospheric pressure, for the wide range of $D/d = 9.6$ to 57.1 and $u = 0.33$ to 13.7 m/s to measure the CHF data in the *L*-regime and check the applicable limit of equation (1) and proposes a generalized correlation predicting the CHF in the *L*-regime.

2. EXPERIMENTAL APPARATUS AND MEASURING METHOD OF CHF

A main part of the experimental apparatus is shown schematically in Fig. 1. Liquid is supplied from a tank (4) through a pump (14) and then to an overflow tank (15) only in the case of the low-speed jet ranging from 0.3 to 4 m/s. It then proceeds to a nozzle (8) and heated by an auxiliary heater (6) as well as a temperature regulator (9) up to the temperature which is always kept below 3 K as compared with the saturation temperature.

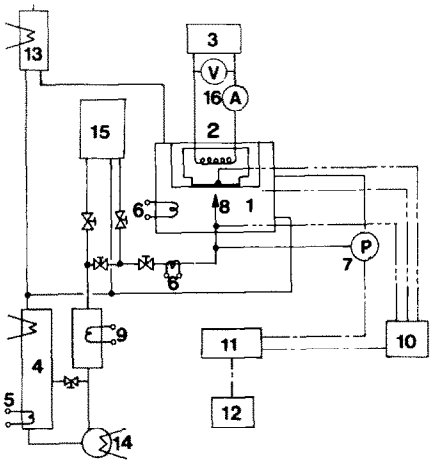

FIG. 1. Whole system of experimental apparatus.

The essential part of the experimental apparatus, shown in Fig. 2, consists of a boiling vessel (1), a copper block (4), and a circular nozzle (6). The boiling vessel is designed to keep the interior saturation temperature at atmospheric pressure. The nozzle is placed in front of the heated surface at the distance of 3 mm by controlling the height adjustment screw (11). The end surface of the

NOMENCLATURE

D	diameter of a heated disk
d	diameter of an impinging jet
g	gravitational acceleration
H_{fg}	latent heat of evaporation
k	constant
q	heat flux
q_{co}	critical heat flux for saturated boiling
ΔT_{sat}	superheated temperature of heated surface ($= T_w - T_{sat}$)
T_{sat}	saturation temperature
T_w	temperature of heated surface
u	velocity of a liquid jet at nozzle exit.

Greek symbols

ρ_l	density of liquid
ρ_v	density of vapor
σ	surface tension.

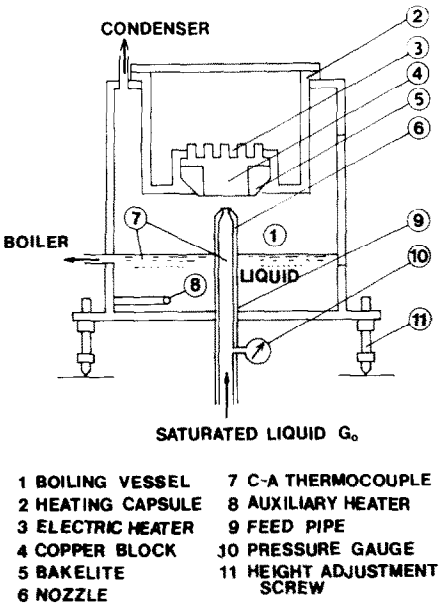

FIG. 2. Main part of experimental apparatus.

cylindrical part of the copper block, which is heated by electric plate heaters mounted in grooves of the copper block and located downwards at the center position in the boiling vessel, provides a circular heated surface. The electric heaters are capable of providing the maximum heat flux of 5 MW/m^2 across the heated surface.

Experiments using water and R113 as the test liquid were made for five different jet diameters (d = 0.7, 1.1, 2.0, 3.35 and 4.13 mm) and two different heated disks (D = 40 and 60 mm) and the jet velocity at the nozzle exit ranging from u = 0.33 to 13.7 m/s. For the 0.7 mm diameter nozzle, no experiment for D = 60 mm is made because the liquid film formed on the heated disk after the impingement of the liquid jet does not cover the entire heated disk at jet velocities below 3 m/s.

The temperature of the heated surface, T_w, as well as the heat flux across the heated surface, q, is determined by means of the three chromel-alumel thermocouples of 0.1 mm diameter set up at regular intervals along the axis of the cylindrical part of the copper block. The actual thermal conductivity of the copper block employed, which must be known to calculate the heat flux, has been carefully determined in the preliminary experiment in the same way as that of Monde and Katto [2]. The velocity of the liquid jet can be accurately determined by measuring the pressure difference between a pressure gauge (10) and the inside of the boiling vessel (1) in Fig. 2 if the discharge coefficient of the nozzle has been determined in a preliminary experiment.

The critical heat flux is determined by the following means: we increase the input to the heater in the copper block in increments that are less than 3% of each preceding heat flux and finally reach the point at which the heated surface temperature runs away. At that point, the CHF is determined within an error of 3%.

3. EXPERIMENTAL DATA

3.1. *Boiling heat transfer*

Figure 3 shows the typical data for fully-developed nucleate boiling obtained in the present experiment. The solid line in Fig. 3 is the result of the nucleate boiling curve obtained by Monde and Katto [2] for a saturated convective boiling with an impinging jet of R113 of velocity u = 1 to 25 m/s. In addition, approximately speaking, this curve is in tolerant accord with a monotonic extension of the nucleate boiling curve obtained in the region of high heat flux of

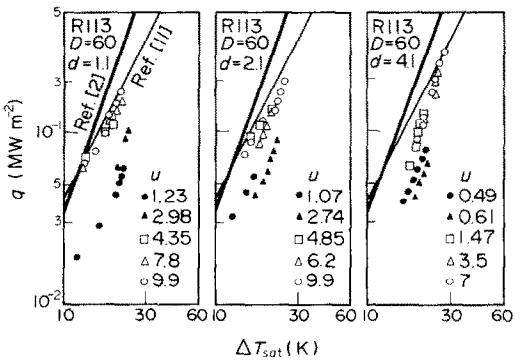

FIG. 3. Saturated nucleate boiling data.

ordinary pool boiling. A light solid line in Fig. 3 represents the nucleate boiling curve obtained experimentally by Ruch and Holman [11] for R113 on the boiling system with a jet impinging upwards on the heated surface.

Apart from the scattering of the data inherent in nucleate boiling, Fig. 3 shows that the measured data are divided into two groups by the jet velocity and the diameter ratio. The data given by the marks ○, □ and △ in Fig. 3 are in a good accord with the Ruch and Holman boiling curve but shift a bit to the high superheated temperature region as compared with the Monde and Katto curve. The reason for this deviation may be that the temperature of the heated surface tends to be estimated a bit lower than the actual temperature due to the employment of the end surface of the conical copper block as the heated surface. Roughly speaking, the nucleate boiling state, as shown by marks such as ○, □ and △ in Fig. 3, can reach a fully-developed state so that it is no longer affected by forced convection. On the other hand, the data given by the marks ● and ▲ considerably deviate from both the boiling curves. This tendency becomes marked with any increase in D/d.

3.2. *Critical heat flux*

Figure 4 shows the CHF data, for example of R113, plotted against the jet velocity u. The solid lines in Fig. 4 are the prediction of equations (1) and (2). The CHF data are proportional to the velocity at low velocity, while about cube root of the velocity at high velocity. It is worth while noting that the CHF data proportional to the velocity correspond to the data of the region represented by the marks ● and ▲ in Fig. 3. We call the CHF proportional to the velocity, the CHF in the L-regime, while the CHF nearly to the cube root of the jet velocity, the CHF in the V-regime.

3.3. *Visual observation of behavior of liquid*

Figure 5 shows behavior of fluid on the heated surface corresponding to the data given by the solid marks in Fig. 3, namely in the L-regime.

As shown in Fig. 5, the heat seems to be transferred by the evaporation from the very thin liquid surface which covers the environs of the heated surface at high heat fluxes. On the other hand, the heated surface near the center is still covered with a thick liquid film where the

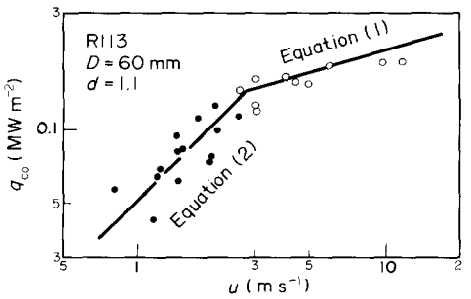

FIG. 4. Critical heat flux data.

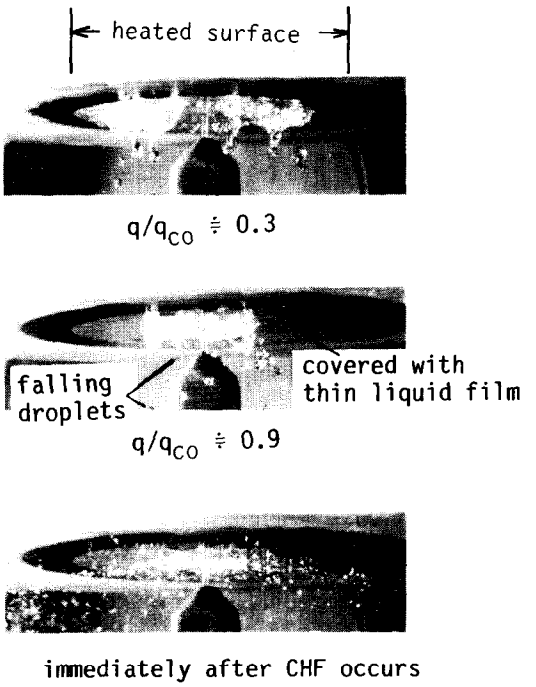

FIG. 5. Aspect of saturated boiling for R113 on downward-facing heated surface (D = 60 mm, d = 1.11 mm and u = 1.23 m/s).

falling droplets as well as a few splashed droplets occur because of the violent nucleate boiling. It might be helpful to take account of the thickness of this thin liquid film. For the sake of simplicity, we choose the typical situation from the boiling curve in Fig. 3, that is, the heat flux of $q = 0.1$ MW/m^2 at the superheated temperature of 20 K. In order to transport this heat flux only by heat conduction through the liquid film of R113 and then by evaporation on its surface, its thickness must be below $\delta = 0.018$ mm. According to the Katto and Haramura model [12, 13], for the CHF mechanism in the V-regime (see Fig. 6 (upper section), [10]), the critical thickness of this liquid film, which plays an essential role in their model for the CHF mechanism, becomes $\delta = 0.146$ mm at the same condition. On comparison of both thicknesses, the characteristic of CHF in the L-regime may be different from the CHF mechanism in the V-regime. A flow model illustrated in Fig. 6 is assumed for the L-regime, where the boiling on the heated surface is suppressed by the thin liquid film [14] and CHF is caused by the dryout of the liquid film. It is very difficult to understand the mechanism of feeding the liquid into such a thin liquid film. It should be noted, however, that it exists on the heated surface on the basis of visual observation.

4. CORRELATION OF CRITICAL HEAT FLUX

4.1. *Critical heat flux in the* V*-regime*

Figure 7 shows, for example, $q_{co}/\rho_v H_{fg} u$ of R113 measured for $D/d > 36$ plotted against $2\sigma/\rho_l u^2(D-d)$

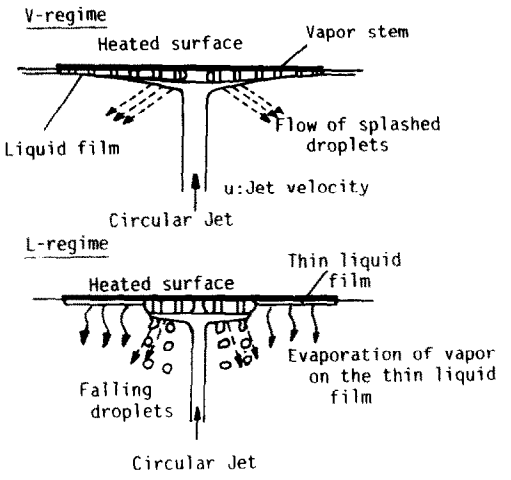

FIG. 6. A flow model near critical heat flux.

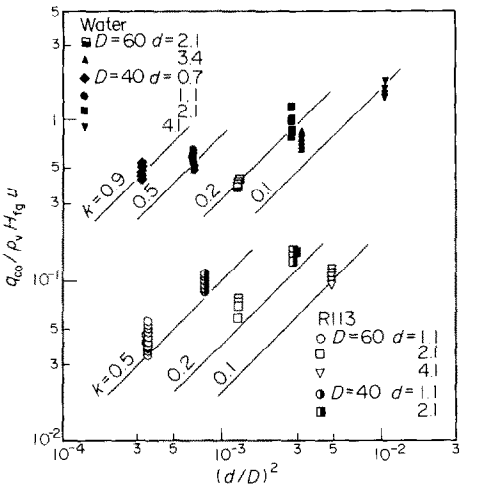

FIG. 8. Effect of $(d/D)^2$ on CHF data.

based upon equation (1), because equation (1) has been proved to be applicable to the CHF for $D/d < 36$ [10]. The CHF in the L-regime is given by the marks ○ and □ in Fig. 7.

Figure 7 shows that equation (1) predicts the CHF in the V-regime with good accuracy but does not apply the CHF with the increase in $2\sigma/\rho_l u^2(D-d)$. In the case of $D/d = 54.1$, for example, equation (1) cannot predict the q_{co} data for $2\sigma/\rho_l u^2(D-d) > 5\times 10^{-5}$.

4.2. *Critical heat flux in the* L*-regime*

On the basis of visual observation of the behavior of the fluid and the boiling curve, the CHF in the L-regime seems to be related to the liquid supply via a heat balance as follows:

$$\frac{q_{co}}{\rho_v H_{fg} u} = k(\rho_l/\rho_v)(d/D)^2 \qquad (2)$$

where k is a fraction of liquid consumed by evaporating on the heated surface to the liquid fed by the impinging jet.

As for the fraction of k, Monde [3], Katto and Kunihiro [4] and Katto and Shimizu [5] reported that in the special case of D/d being very large, this kind of CHF should appear but was not established by their experiment, so that $k = 1$ was assumed for simplicity. On the other hand, this phenomenon was observed by Monde [15] who carried out a study of CHF in a saturated, forced convection boiling with impinging droplets, as well as by Kopchikov *et al.* [16], who conducted an experiment of mist cooling employing droplets supplied through a vertical spray nozzle. Though both boiling systems were different from the present system, Monde obtained $k = 0.8$, while Kopchikov obtained $k = 1.0$.

Figure 8 shows $q_{co}/\rho_v H_{fg} u$ plotted against $(d/D)^2$. The k values on each line are calculated from the experimental data using equation (2). As shown in Fig. 8, one notes that the k values for the same nozzle diameter are nearly equal, and then become large with any decrease in the nozzle diameter. Figure 9 shows the relationship between $1/k$ and d. It is found from Fig. 9 that $1/k$ is given as a function of d. The k value seems to be related to the falling droplets from the liquid film (*cf.* see Fig. 5). The k value may be associated with the two nondimensional parameters $(\rho_l/\rho_v,\ d/\sqrt{\sigma/g(\rho_l-\rho_v)})$, which govern the Taylor instability of a liquid film. It should be noted that the nozzle diameter, d, may be indirectly connected as the physical property relating to the thickness of the liquid film. The function of k can

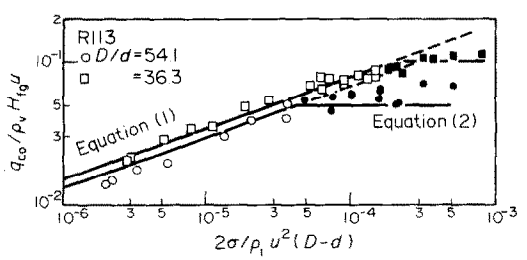

FIG. 7. $q_{co}/\rho_v H_{fg} u$ versus $2\sigma/\rho_l u^2(D-d)$.

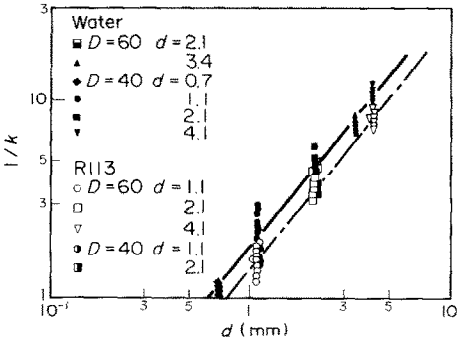

FIG. 9. $1/k$ versus d.

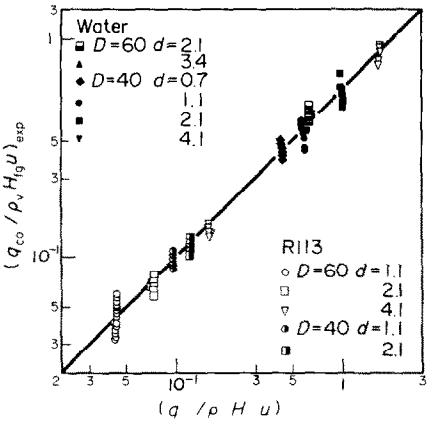

FIG. 10. Nondimensional correlation of CHF.

be given using the two nondimensional parameters as:

$$\frac{1}{k} = C(\rho_l/\rho_v)^m(d/\sqrt{\sigma/g(\rho_l-\rho_v)})^n. \quad (3)$$

The constant C and the powers m and n can be determined by means of the least squares method to combine the two groups of the CHF data (water and R113) in Fig. 9 into a single group to give $C = 3.89 \times 10^{-2}$, $m = 0.674$ and $n = 1.24$. Equation (3) becomes as follows:

$$\frac{1}{k} = 3.89 \times 10^{-2}(\rho_l/\rho_v)^{0.674}(d/\sqrt{\sigma/g(\rho_l-\rho_v)})^{1.24}. \quad (4)$$

Figure 10 shows the CHF data as compared with that predicted by substituting equation (4) into equation (2).

The k value is apt to change for the upward facing heated surface. So, it should be hoped to check the k value by making the experiment for the direction of the heated surface other than downwards.

5. BOUNDARY BETWEEN *L*- AND *V*-REGIME

The boundary between L- and V-regime, where q_{co} is continuous, may be determined by eliminating q_{co} from equations (1) and (2) as,

$$(d/D)^2(1+D/d)^{0.364} = 8.60 \times 10^{-3} \times (\rho_l/\rho_v)^{0.319}(d/\sqrt{\sigma/g(\rho_l-\rho_v)})^{1.24} \times (2\sigma/\rho_l u^2(D-d))^{0.343}. \quad (5)$$

As the CHF in the L-regime generally takes place at $D/d > 10$, $(1+D/d)^{0.364}$ in equation (5) can be equal to $(D/d)^{0.364}$ so that equation (5) becomes as follows:

$$D/d = 18.4(\rho_l/\rho_v)^{0.194} \times (d/\sqrt{\sigma/g(\rho_l-\rho_v)})^{-0.76} \times (2\sigma/\rho_l u^2(D-d))^{-0.209}. \quad (6)$$

For simplicity, we deal with the case of $d = 1$ mm because the possibility for appearance of the CHF in the L-regime becomes high with the decrease in d. Figure 11 shows, for example, the boundary line for R113 is the prediction of equation (6) for $d = 1$ mm, while a dot–dash line is predicted for $d = 1$ mm by equation (5). The marks ○ and ● in Fig. 11 represent the CHF data for R113 in the V- and L-regimes, respectively.

6. CONCLUSIONS

(1) The CHF in the L-regime appears only when the jet velocity is very small and in addition the diameter ratio, D/d, is very large.

(2) The CHF is predicted by equation (2) with good accuracy, which is introduced by equalling the liquid supply to that consumed by evaporation on the heated surface.

(3) The boundary between L- and V-regimes is given by equation (6).

Acknowledgement—The authors would like to acknowledge Prof. Y. Katto, University of Tokyo and Prof. H. Kusuda, Saga University for their helpful advice. The authors also express their appreciation to Messrs. M. Daigen and N. Shigematus for their valuable assistance with the experiment. The Ministry of Education, Science and Culture is acknowledged for the financial support to this study under Grant in Aid of Encourage Research No. 56750142.

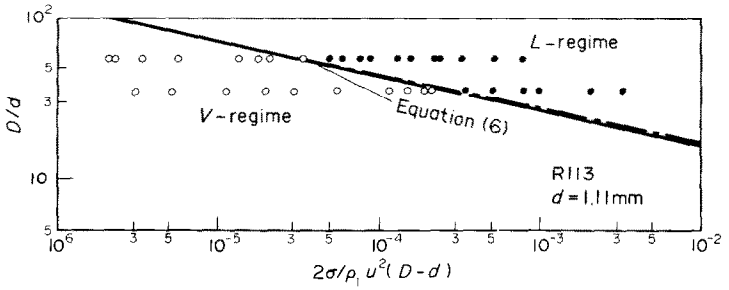

FIG. 11. Boundary between CHF in the L- and V-regimes.

REFERENCES

1. Y. Katto and M. Monde, Study of mechanism of burnout in a high heat-flux boiling system with an impinging jet, *Proc. of the 5th Int. Heat Transfer Conference, Tokyo*, Vol. IV, pp. 245–249 (1974).
2. M. Monde and Y. Katto, Burnout of a high heat-flux boiling system with an impinging jet, *Int. J. Heat Mass Transfer* **21**, 295–305 (1978).
3. M. Monde, Burnout heat flux in saturated forced convection boiling with an impinging jet, *Heat Transfer—Jap. Res.* **9**(1), 31–41 (1980).
4. Y. Katto and M. Kunihiro, Study of the mechanism of burnout in boiling system of high burnout heat flux, *Bull. JSME* **16**, 1357–1366 (1973).
5. M. Katsuta, Boiling heat transfer of thin liquid film with an impinging jet, *Proc. of the 14th Nat. Heat Transfer Symp. of Japan*, pp. 154–157 (1980).
6. M. Katsuta, Boiling heat transfer of thin liquid film with an impinging jet, *Preprint of JSME* **780**(18), 68–70 (1978).
7. Y. Katto and M. Shimizu, Upper limit of CHF in the forced convection boiling on a heated disk with a small impinging jet, *J. Heat Transfer* **101**(2), 265–269 (1979).
8. J. H. Lienhard and R. Eichhorn, On predicting boiling burnout for heaters cooled by liquid jets, *Int. J. Heat Mass Transfer* **22**(5), 774–776 (1979).
9. J. H. Lienhard and M. Z. Hasan, Correlation of burnout data for disk heaters cooled by liquid jets, *J. Heat Transfer* **101**(2), 383–384 (1979).
10. M. Monde, Critical heat flux in saturated forced convective boiling on a heated disk with an impinging jet, *Wärme-u. Stoffüberstr.*, in press.
11. M. A. Ruch and J. P. Holman, Boiling heat transfer to a Freon-113 jet impinging upward onto a flat heated surface, *Int. J. Heat Mass Transfer* **18**(1), 51–60 (1975).
12. Y. Haramura and Y. Katto, A new hydrodynamic model of critical heat flux, applicable widely to both pool and forced convection boiling on submerged bodies in saturated liquids, *Int. J. Heat Mass Transfer* **26**(3), 389–399 (1983).
13. Y. Katto, Critical heat flux in forced convection flow, *Proc. of ASME–JSME Thermal Engng. Joint Conference*, Vol. 1, pp. 1–10 (1983).
14. L. S. Tong, *Boiling heat transfer and two-phase flow* (Chap. 5, Flow boiling), p. 119. John Wiley & Sons (1965).
15. M. Monde, Critical heat flux in the saturated forced convection boiling on a heated disk with impinging droplets, *Heat Transfer—Jap. Res.* **8**(2), 54–64 (1980).
16. I. A. Kopchikov *et al.*, Liquid boiling in a thin film, *Int. J. Heat Mass Transfer* **12**, 791–796 (1969).

FLUX CRITIQUE DANS L'EBULLITION EN CONVECTION FORCEE SATUREE SUR UN DISQUE CHAUFFE ET UN JET INCIDENT-CHF EN REGIME L

Résumé—Une étude expérimentale du flux thermique critique (CHF) est décrite pour un système saturé et convection forcée à pression atmosphérique : un liquide d'eau ou de R 113 sortant en un jet mince et circulaire, frappe un disque chauffé. Les expériences sont conduites pour une vitesse $u = 0{,}33$ à $13{,}7\ \mathrm{m\,s^{-1}}$ et un rapport de diamètre $D/d = 9{,}6$ à $57{,}1$. Le CHF qui apparait dans ces conditions est divisé en deux régimes caractéristiques différents (L et V) dépendants de la vitesse du jet, du rapport des diamètres et du diamètre du jet. Le CHF dans le régime L, pour une vitesse faible et un grand rapport de diamètres qui avait été imaginé jusqu'ici mais jamais prouvé expérimentalement, est non seulement obtenu mais aussi précisé par une formule générale, avec une bonne précision.

KRITISCHE WÄRMESTROMDICHTE BEIM SIEDEN IN GESÄTTIGTEN SYSTEMEN BEI ERZWUNGENER KONVEKTION AN EINER BEHEIZTEN SCHEIBE MIT EINEM AUFTREFFENDEN STRAHL—CHF IM L-REGIME

Zusammenfassung—Es wurde eine experimentelle Untersuchung der kritischen Wärmestromdichte (CHF) bei erzwungener Konvektion in gesättigten Systemen unter Atmosphärendruck durchgeführt. Flüssigkeit wird durch einen kleinen, runden Strahl aus Wasser oder R 113 zugeführt, der von unten auf eine beheizte Scheibe auftrifft. Die Experimente wurden durchgeführt für eine Geschwindigkeit $u = 0{,}33$ bis $13{,}7\ \mathrm{m\,s^{-1}}$ und ein Durchmesserverhältnis von $D/d = 9{,}6$ bis $57{,}1$. Die kritische Wärmestromdichte, welche in dem vorliegenden experimentellen Bereich auftritt, wird in zwei verschiedene charakteristische Regime (L- und V-Regime) eingeteilt, welche von der Strahlgeschwindigkeit, dem Durchmesserverhältnis und dem Strahldurchmesser abhängen. Die kritische Wärmestromdichte im L-Regime ist nicht nur im vorliegenden Experiment gefunden worden, sondern auch durch eine allgemeine Korrelation mit guter Genauigkeit vorausgesagt worden.

КРИТИЧЕСКИЙ ТЕПЛОВОЙ ПОТОК ПРИ КИПЕНИИ В СЛУЧАЕ ВЫНУЖДЕННОЙ КОНВЕКЦИИ В УСЛОВИЯХ НАСЫЩЕНИЯ НА НАГРЕТОМ ДИСКЕ С УДАРЯЮЩЕЙСЯ О НЕГО СТРУЕЙ—КТП В L-РЕЖИМЕ

Аннотация—Экспериментально изучен критический тепловой поток (КТП) в случае вынужденной конвекции для системы в условиях насыщения при атмосферном давлении, при этом жидкость подавалась в виде небольшой круглой струи воды или хладагента R113 к нагретому диску. Эксперименты проводидись для скорости u от 0,33 до 13,7 м/с и отношении диаметров D/d от 9,6 до 57,1. Для существующего в исследуемом диапазоне КТП имеют место два различных характерных режима (L- и V-режимы), зависящих от скорости, отношения диаметров и диаметра струи. КТП в L-режиме (при довольно малой скорости и большом отношении диаметров), появление которого предполагалось, но не было доказано экспериментально, был не только получен в настоящем эксперименте, но и предсказан с помощью обобщенных уравнений с хорошей точностью.